Design and Shape Optimization of Aerostat Envelopes

Amool A Raina *Project Engineer,* ***Rajkumar S. Pant*** *Associate Professor*

Aerospace Engineering Department,

Indian Institute of Technology Bombay, Mumbai Maharashtra, 400076, India

Abstract

The paper provides details of a methodology for design and performance analysis of the aerostat. The methodology is a systematic collation of various design approaches and concepts, which were examined during the ongoing design and field trial exercises related to remotely controlled airships and aerostats at the Lighter-Than-Air Systems Laboratory of IIT Bombay. A methodology for arriving at the size of fins from static stability considerations is presented, which includes determination of tether profile. The various design decisions were driven by the availability of local materials for different components.This paper outlines a Multi-disciplinary Optimization approach for identifying the optimum shape of an aerostat envelope that results in the largest payload capacity for a given envelope volume. Apart from aerodynamics, the participating disciplines in this optimization problem are flight mechanics and structures. Some constraints that take into consideration the difficulty in fabrication of certain kinds of shapes have also been included. A shape generation algorithm for parameterization of a general envelope shape in terms of standard geometrical surfaces is then described. The problem is posed in an optimization framework and optimum shapes are obtained using Genetic Algorithms. Results for an aerostat of envelope volume of 2000 m^3 reveal that the payload capacity of the optimum shape of single fabric construction is ~ 2.2 % higher compared to a similar envelope using the standard GNVR shape. However, use of multi-fabric construction was seen to increase the payload capacity by ~ 22% for both the GNVR and optimum shape. Sensitivity analyses revealed that the payload capacity decreases considerably with increase in fabric density, and tether weight per unit length due to increased self weight, and angle of attack. It was also seen that the fin weight and the location of confluence point depend to a great extent, on the location of CG.

Nomenclature

AGL	=	Above Ground Level
CB	=	Centre of Buoyancy
C_{DV}	=	Volumetric drag coefficient
CG	=	Centre of gravity
C_p	=	Pressure coefficient
d	=	Diameter of the envelope [m]
D	=	Drag on the envelope [N]
GNVR	=	*GNV Rao envelope Profile for aerostat*
l	=	Length of the envelope [m]
LOS	=	Line of Sight
$Lift_{net}$	=	Net lift [kg]
LMDS	=	*Local Multipoint Distribution System*

PADS	=	Procedure for Aerostat Design and Sizing
Pu_{LTA}	=	Percentage purity of the contained gas [%]
Pr_{aero}	=	Pressure due to aerodynamic loading (kg/m^2)
Pr_{hydro}	=	Pressure due to Dynamic Pressure loading (kg/m^2)
Re	=	Reynolds number
$a_1, b_1, c_1, d_1, a_2, b_2, c_2, d_2$	=	Coefficients of cubic splines that parameterize middle portion of envelope
a_n	=	Coefficient for parabolic rear shape
C_{m_α}	=	Change in moment coefficient with angle of attack (Stability margin)
$d_{\max}$	=	max. diameter of aerostat envelope
F_{comp}	=	Composite Objective Function
$(\overline{x_c}, \overline{z_c})$	=	Coefficients of confluence point
P_R	=	Internal overpressure in the aerostat envelope
R	=	Radius of curvature of spherical front portion
S	=	surface area
t	=	envelope material thickness
X_D	=	Six dimensional design vector
$y_{\max}$	=	maximum radius of aerostat envelope
ρ_{matl}	=	Area density (weight per unit area) of envelope material
σ_{max}	=	maximum stress
$\sigma_1, \sigma_2, \sigma_3$	=	maximum stress limit of Fabric # 1,2 & 3, respectively

I. Background and Introduction

An aerostat is an aerodynamically shaped tethered body, belonging to the family of Lighter-than-air vehicles. Aerostat envelopes are filled with a 'lighter than air' gas (which is Helium or Hydrogen in most cases) and thus generate lift due to buoyancy. The envelope is gimbaled at the tether confluence point, so that it can freely align with the direction of the ambient wind. Adequately sized fins are provided on the envelope to impart it stability during wind disturbances. Payloads in modern day aerostats are usually radars, surveillance cameras or communication equipment. In order to deploy more sophisticated equipment on Aerostats, it is always desirable to increase their payload capacity, without compromising on their operating altitude. This paper also provides details of a methodology for arriving at the optimum shape of the envelope of an aerostat, keeping in mind the aerodynamic and structural considerations, while incorporating some constraints imposed from manufacturing considerations.

II. Aerostat Design Methodology

Depending on the payload, range of surveillance, and operational time at station, aerostats have been launched to an operating altitude of around 4600 m from sea level. As per published literature from Ref. 17, aerostats have been successfully deployed by commercial companies to carry payload such as Surveillance radars of all sizes and capabilities, Signal Intelligence (SIGINT) collection equipment, Gyro-stabilized daylight,

low-light level and infra-red video cameras, Direct television broadcast and relay, FM radio broadcast and relay, VHF/UHF, Ground Control Intercept (GCI) and microwave communications, and Environmental monitoring equipment.

Based on the preliminary work carried out by Gupta & Pant[1], and Raina & Gawale[2], a methodology for initial sizing and conceptual design of an aerostat system has been developed to arrive at the required geometrical parameters and detailed mass breakup of an aerostat system, given the values of some operation, configuration, and performance related parameters. This methodology implements spread sheet form of MS-EXCEL™ and named as PADS.

PADS accepts all the input parameters, constant parameters, and some geometrical and operation related options such as envelope profile selection, gas pressure management by ballonets or symmetrically expandable elastic strip, and type of LTA gas used. The objective behind providing this facility for selection of optional parameters was to make the methodology more flexible and adaptive for any future modification in the aerostat system, and also to make sensitivity analyses much more comprehensive.

In an aerostat the geometry of the envelope has a profound effect on its aerodynamic characteristics, and hence on the stability and payload carrying ability. Some standard shapes of the aerostat envelopes exist and their profiles were incorporated in the input part of the PADS. A brief overview is given in the section that follows:

A. Various modules in PADS

PADS is designed in a modular fashion and contains 48 spread sheets with separate modules that cover the calculations related to LTA gas properties in the atmosphere, and sizing of envelope, petal, tether and fins. It also has modules that carry out calculations related to LOS error angle calculation, pivot and safety-system attachment. The fabrication process plans, including that of a small winch are worked out and cost calculations are carried out. Design flow is described in a modular way which enables to understand the contribution of each module for the design and sizing in subsequent steps.

B. Design Requirements

The main module is the heart of PADS, all the inputs and options can be selected to perform design and analysis. Table 1 shows a typical structure of the spread sheet for input parameters. PADS is designed for SI units.

Table 1: Sample inputs of Main module of the PADS

Input Parameters	SI Unit	Typical Value
Payload	[kg]	7.00
Floating Altitude (From Sea Level)	[m]	740.81
Spot Altitude from Sea Level	[m]	560.00
Design Wind Speed	[m/s]	15.00
Off Standard Temperature	[^{o}C]	20.00
Operational Time	[days]	15.00
Diurnal Temperature range	[^{o}C]	10.00
Free Lift Permissible	%	15.00
Permissible Reduction in Altitude	±DH	5.00

Constant Parameters		
Contained Gas Initial Purity	[%]	99.50
Option for Envelope Material (PVC-1, Other-2)	PVC	1.00
Rate of Gas Permeability thru Envelope fabric	[ltr/m^2/day]	2.50
PoE Cable Specific Length	[kg/m]	0.04
Low Loss Cable Specific Length	[kg/m]	0.00
Elastic Strip Specific Length	[kg/m]	0.02
Available PVC Fabric density	[kg/m^2]	0.21
Permissible Blow by and Excess Length for all the cables Design altitude AGL	%	20.00
Centre of pressure for Aerostat (0.3-0.35)	[-]	0.33
Options		
Profile Configuration (NPL-1, GNVR-2, SAC-3, Optimum-4, TCOM360Y-5)	SAC	3
Petal Configuration (1-Single, 2-Double)	Double	2
Rear Gore Petals (No. of Petals)	[-]	10.00
Front Gore Petals	[-]	20.00
Contained Gas (He-1, H2-2)	Helium	1
Include Integrated Balloonet OR Elastic Strips (Ballonet-1,El Strip-2)	El. Strip	2
Fin fabrication (Inflatable-1, Rigid outline with cover-2)		1
Mass specific length of the 0.5 inch PVC pipe	gm/m	125.00

The spreadsheet like form of PADS also helps in carrying out extensive sensitivity studies. In order to resize the aerostat of a given configuration and material for different operating conditions, only the operating parameters have to be changed. The Main module in the PADS is linked to other modules for design and sizing of various components of the Aerostat; this includes Atmosphere, Envelope, Fin, Petals for the envelope, Pivot and safety, and accessories such as winch. The required output/s from these modules is posted back to Main module.

C. Envelope sizing, estimation of net Lift and Drag

PADS starts by inputting all the required input data as mentioned in the Table 1. A starting value for the envelope length is specified which keeps on changing until the total aerostat empty weight is balanced by payload and free lift. Each instantaneous length taken by PADS invokes the envelope sizing module to multiply the same to the normalized coordinates of the selected profile from Database and Options module. With numerical integration method, program calculates the volume and surface area of selected profile; this in turn used to calculate CG and CB. A detailed layout of the envelope profile, reference fin geometry and the single gore petal is collectively shown in the Fig. 1. All the features shown are gathered from different modules.

The Atmosphere module starts calculating the required off standard air properties not only at the design altitude, but also at the permissible vertical drift altitude, and at ground level by considering the pressure, temperature and density at ISA conditions

This module also calculates the Dynamic viscosity and Reynolds number at the design altitude. All the required formulae to calculate these air properties are taken from Anderson[3] and Khoury & Gillett[4]. Similarly, properties of the selected L-T-A gas are also calculated at respective altitudes.

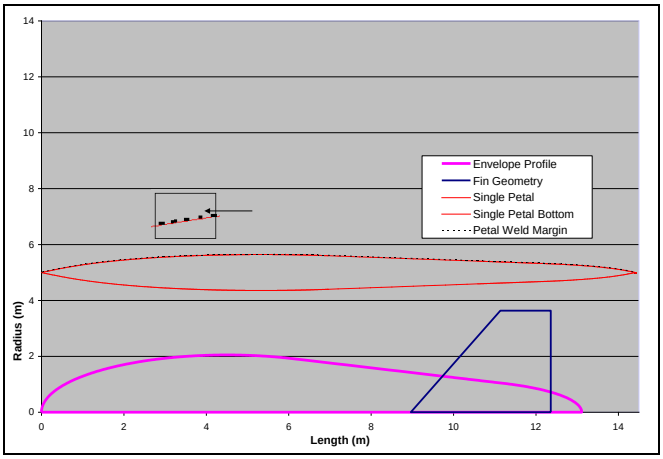

Figure 1. PADS generated combined output for envelope profile and reference fin geometry (Ref. 7)

Figure 2. An inflated 100m^3 envelope of the aerostat

The Main Module receives the required properties of air and LTA gas and calculates the net disposable lift with volume of envelope, purity of LTA gas as per Eq. 1 from Ref. 4. According to Hoerner[5], the aerostat envelope contributes heavily to its drag, exceeding over 60-70 %. In order to seek the drag of the aerostat like body where lift is directly related to the volume; C_{DV} is calculated as per Eq. 2 taken from Ref. 4.

$$Lift_{net} = V_e \times \left[\rho_{air} - \left(\rho_{LTA} \cdot \left(\frac{Pu_{LTA}}{100} \right) + \left(1 - \left(\frac{Pu_{LTA}}{100} \right) \right) \cdot \rho_{air} \right) \right] \quad \text{Eq. (1)}$$

$$C_{DV} = \left[0.712 \cdot \left(l/d \right)^{1/3} + 0.252 \cdot \left(d/l \right)^{1/2} + 1.032 \cdot \left(d/l \right)^{2.7} \right] \cdot \mathrm{Re}^{-1/6} \quad \text{Eq. (2)}$$

Drag on the envelope is calculated using Eq. 2 and Eq. 3.

$$D = \frac{1}{2} \cdot \rho_{air}^{a} \cdot v^2 \cdot V^{2/3} \cdot C_{DV} \quad \text{Eq. (3)}$$

This value is used in tether module along with other parameters for calculating the expected blow by which is explained later.

D. Internal Over Pressure Estimation

In order to maintain positive pressure inside the envelope, three main loadings are considered to estimate the internal over pressure (ΔP) viz., the loading due to dynamic pressure, aerodynamic loading, and hydrostatic pressure as suggested by Gupta & Malik[6].

Since the aerostat envelope diameter is more than twenty times of the thickness of the material; it can be considered as a very thin shell and hence hoop stress is calculated in terms of the circumferential unit load as shown in Eq. 4.

$$\sigma_c = \Delta p \cdot \frac{d}{2} \qquad \text{Eq. (4)}$$

Normally, this value is expressed in terms of kg/5cm of circumferential length of maximum diameter of envelope material fiber. This gives the allowable load that the envelope material fiber of 5 cm length, aligned in circumferential fashion can bear. The stress calculated using Eq. 4 is then compared with the allowable stress value of the selected fabric stored in the database. A factor of safety of 4 (four) has normally been kept in selection of envelope fabric. This is required to take care of the inaccuracies in the calculation of diurnal temperature variations, degradation in the envelope material due to handling and prolonged exposure to atmospheric conditions, and changes in gas properties due to superheat.

E. Gore petal sizing

In most of the aerostats, petals are shaped depending on size of the envelope and the available form of material. In India, PVC rolls are usually available in a flat pipe form (double layers) of 26" width with 50 ft length. In order to achieve more accurate shape after inflation, a large number of petals are employed, if the welding length is not a constraint. For operational benefits, however, a wider material with fewer welds is always preferable from leakage view point.

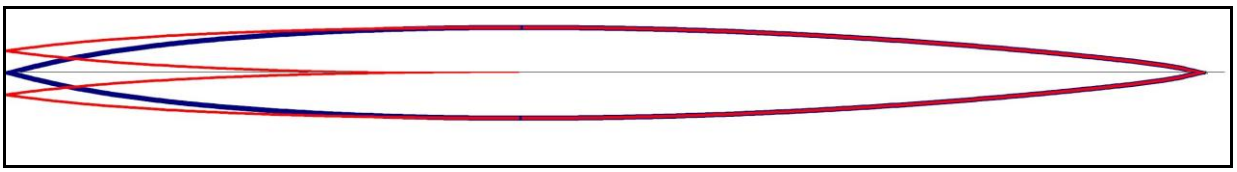

Figure 3. Conceptual sketch of single and split petal for envelope fabrication

But lesser number of petals leads to an improper shape of the envelope, especially at the ends. Usually less petals and greater curvatures at the nose portion, lead to many folds and thus affects the shape of the envelope and also the surface quality. In order to reduce these folds, a novel technique is incorporated as suggested by Gupta & Malik[6], in this technique; a single petal is divided at certain appropriate location near the maximum diameter (normally 40% from the nose) in to two symmetric petals as shown in Fig 3. Thus, a single petal remains single at maximum diameter and subsequently at rear ends, in the region of maximum diameter, and

also gets double at the nose portion to avoid folds. This split technique ensures weld joints only in front area and thus leads to minimum weld lengths.

F. Fin Sizing

Fin module of PADS accepts the fin sizing parameters as soon as the selected envelope is scaled to inputted length in envelope sizing module. PADS's fin sizing and mass estimation are based on the reference fin area. Based on the selected profile from Database module, a ratio of each part of the fin geometry to the envelope length (Root chord, Tip chord, Average half span, and the location of the trailing edge from the nose of the aerostat, to the length of the aerostat) is calculated. A linear scaling is performed on all the parameters so as to get the exact plan form geometry of the fin for the instantaneous envelope length. PADS does the fin sizing structurally for two types of fin, one is the conventional inflatable structure with symmetric airfoil and other is the framed PVC structure. NACA 0018, aerofoil cross section is commonly used as a default cross section for all the fins of various envelope profiles available in the PADS Database and Options module;

Coordinates of this airfoil are extracted from Greschner[7] et. al. and Mason[8].

For an inflatable fin, it is necessary to join the flexible ribs made of the same material as fin to get a reasonably accurate shape of the desired aerofoil cross-section after inflation. As suggested by David[9] et. al.,

Figure 4. Photograph of the Aerostat taken during the field trials conducted at Gliding Centre, Pune displaying the internal structure of the fin.

thirteen ribs were used in the fin structure. The trailing edge can either be cut or can be aligned properly by means of harder plastic so as to maintain the contour.

Two CAD tools viz., AutoCAD2004™ and Solidworks2005™ were used for accurate rib sizing. The entire 3-D fin is firstly converted in to a flat 2-D structure by knowing the perimeter of the profile at both root and tip levels separated by the reference half span. This gives the area which is then multiplied with surface density of cover material to get the mass of the cover. The width of each rib is calculated by dividing the root and tip airfoils at appropriate intervals and getting the local thickness. A margin for weld is always added to this thickness. Length of each rib is calculated directly by joining the rib from tip at one point to the corresponding point at root locations. Thus knowing the length and width at root and tip for each fin, surface area of all the ribs is calculated by multiplying it with the material surface density.

G. Tether sizing and Profile generation

A tether module is developed in PADS to calculate the exact length of the combination of tether and PoE cable required for given design altitude, wind speed, permissible blow by, and permissible free lift in the aerostat at the design altitude. This sizing is based on the method suggested by Wright[10] which determines blow by of the aerostat and tether profile, given the tether tension and the tether angle at the confluence point. In this method, the tether is discretized into elements of equal lengths and starting from the confluence point, the tension and inclination angle of each subsequent element below is determined by solving for the equilibrium of forces as shown in the Fig. 5.

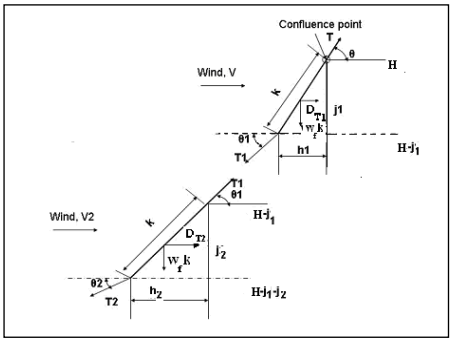

Figure 5. Free body diagram of discretized elements of tether (Ref. 17)

The tether module also predicts the profile taken by the tether at various ambient wind speeds as shown in Fig. 6 in the sensitivity studies performed by PADS. It can be seen that an increase in wind speed increases blow by. It is evident that as the tether is released, the aerostat drifts in the direction of wind due to blow-by; thus tether mass keeps on increasing leading to reduction in the free lift and also in the operating altitude. If, on the other hand, the tether length is maintained constant, the aerostat comes down from its design altitude to balance the forces acting on it. In practice, as suggested by Gupta & Malik[6], 20% extra tether is provided to take care of blow by.

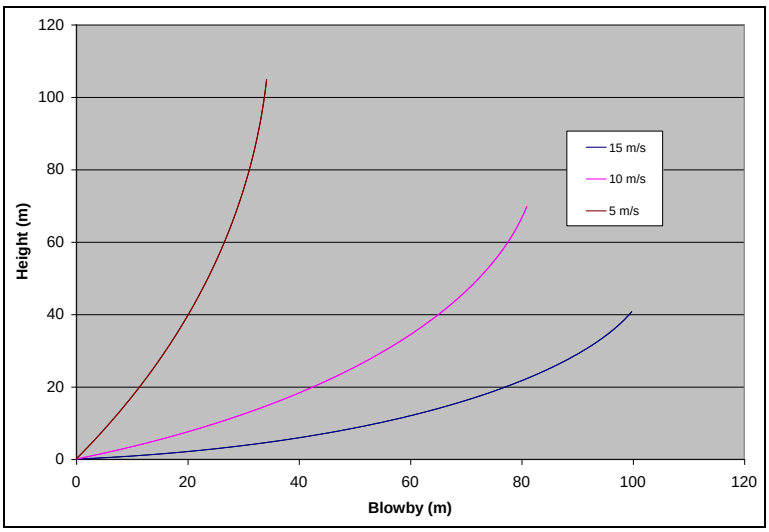

Figure 6. Sensitivity of tether profile with winds

Mass of the tether which is a combination of load and PoE cable is calculated by knowing the length AGL multiplied by the specific mass of the individual cable. Tether module also takes other issues in to account, such as load due to PoE cable, confluence lines to distribute the load on the envelope at various locations, and Pivot frame etc. Confluence lines' mass is taken as 1 % of the envelope mass, and the pivot frame mass is taken after fabrication as per the payload space requirements.

H. Gas pressure management

This module provides two options; the ballonets or Elastic Strips for managing the gas internal over pressure. In case of ballonets, knowing the net positive lift at ground level, the volume of air to maintain aerostat both at ground and design altitudes is calculated. In addition to this volume, some additional air volume is calculated to maintain the platform performance at the design altitude in the effect of diurnal temperature variation at the local condition. Thus, once the total volume of air that is to be available in the ballonets is calculated, material for one or two ballonet bags which are to be kept within envelope for this air is calculated. It is obvious that before ballonet calculation, the volume calculated for the envelope is not enough to raise the

payload to the design altitude. Hence, resizing is carried out by changing length with which envelope was calculated prior to the ballonet sizing.

In case of Elastic strips, sizing and mass estimation is carried out by calculating the expansion of the gas from ground to the design altitude. This varies the maximum diameter circumference which is recorded by Gas pressure management module, with some room for expansion and contraction to take care of the envelope in the diurnal temperature variations.

While launching the aerostat, envelope is filled with the lifting gas slightly less by an amount of expansion till it ascends to the design altitude which is given by the calculations in the Main module. Elastic strips maintain the tightness in the envelope. As it goes up, elastic strips allow the gas to expand and thus envelope remains tight at any altitude within the design range. Thus, knowing the volume at ground level and at design altitude, the required circumference at maximum diameter of the envelope is calculated. The difference in the circumference gives the maximum width of the elastic region, and it is maintained proportionately on front and rear portion of the maximum diameter along the petal profile. Usually the elastic region is kept 30% of the envelope length. The dead length is the length of the elastic strip which gives maximum stretchable length more than that of required circumferential expansion. Thus, width of the maximum expandable length to take care of expansion under circumferential unit load is the sum of difference in circumference of maximum diameter at superheat volume of the envelope to ground level volume plus dead length of the strip depending on the properties. A factor of safety is included knowing the fact that the envelope contraction can be managed but the expansion is quite undesirable. Further, knowing the maximum width and maximum length of the elastic region total length required, specific mass, mass of the hooks to maintain a zigzag fashion in the region and other mass of attachments are calculated.

I. Weight Estimation of Various groups

Main module continues to calculate the total system mass breakdown in terms contained gas, Envelope group, Fin group, tether group, and other accessories group. All the sub group parameters are received from respective module.

PADS calculates weight of rigging, hooks, patches, nose battens and Gas filling hose/port/opening in terms of the percentages of envelope. Table 2 shows the mass breakup of each group and its values for a typical aerostat.

Table2: Mass breakdown for a typical Aerostat System

Group Name	Sub Group	Value kg
	Contained Gas	15.18
Envelope	**Envelope Group**	30.98
	Envelope	26.3
	Rigging, Hooks (24 No.) and Patches (8 No.)	1.58

	Nose Battens	2.63
	Gas Filling Hose/Port/Opening (s)	0.53
Elastic strips	**Elastic Strips group**	2.62
	Mass of the elastic strip	0.91
	Mass of corner hooks	1.61
	Mass of support patch for elastic region	0.10
Fin	**Mass of Fin Group**	13.22
	Mass of PVC Cover	3.65
	Mass of total spars	0.588
	Total fin Mass	4.24
	Total Empennage mass	
Tether	**Tether Group**	23.13
	Tether	10.85
	PoE Cable	8.68
	Pivot with payload frame	3.34
	Confluence lines Support Distribution Wires (1% of Envelope Mass)	0.26
	Other Accessories	0.70
Other	Night Visibility System (Five Pin Lights)	0.50
	GPS Receiver	0.20
	Gross Take off Empty Mass	70.64

J. Winch Design and development:

The winch is designed to arrive at a cost effective design, with main emphasis on local availability of material and fabrication techniques. An 'open ended approach' was used so that it could be continuously upgraded during its development cycle. This work is taken from Sequeira[11] et. al.; the specific design requirements for winch design were arrived from one of the modules described in PADS. This included parameters like expected tether tension, drum size, tether winding rate, and tether profile, power requirements for winding, Tether configuration (combination of Load and data cables, Specific weight, and diameter), minimum bending radius for cable, and length of the tether. With these inputs, main drum with collar at the ends was structurally designed with the suggestions given by Markey[12], by treating it as a simply supported beam with a uniformly distributed load in terms of tether mass, and line pull as a point load. On the same lines, the complete structural design was carried out for spur gears, selection of frame cross section, provision of other drum for data cable etc. A braking system was also designed to regulate the ascending rate of aerostat with a line pull of over 70 kg. An innovative inversion of four bar link mechanism was employed for symmetrical application of the brake pressure by means of two brake shoes; which ultimately results in an effortless braking even by manual means. Fig. 7 shows a conceptual layout of this braking system. Snap shots of the winch in operation are shown in Fig. 8.

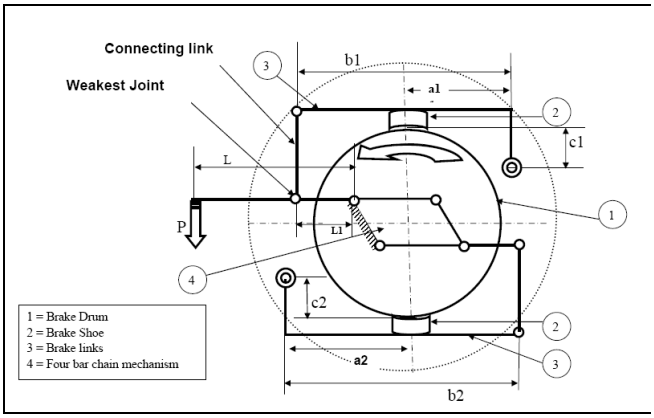

Figure 7. Braking mechanism using inversion of four bar links

When the force P is applied at one end of the link L which is pivoted mainly at fixed link L_1 drives the two links indicated by its length b_1 and b_2. Link b_1 is directly connected whereas b_2 is connected in opposite direction by means of an inversion of four bar link mechanism as shown by number 4 in the Fig. 7. Lengths a1, b1, c1 and a2, b2, c2 are so adjusted that the shoes hinged at b1 and b2 applies almost equal pressure on the drum. Thus the braking mechanism does not create any bending force on the shaft on which it is mounted.

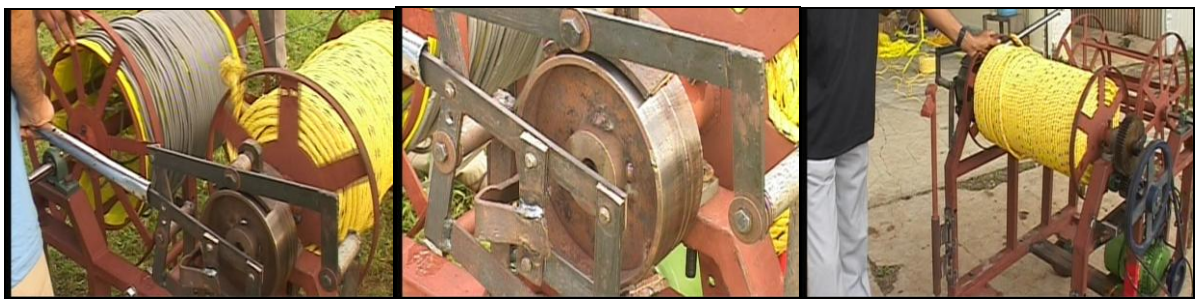

Figure 8. Snap shots of winch in operation during field trials

A field trial revealed that the winch was toppling due to high line pull on the tether due to low weight of the winch. Therefore, a toppling arrester was developed and attached to the winch. This arrester has four studs housed in a barrel which is connected to the frame of the winch at four corners. Once the winch is placed at the launch location, these studs are pierced inside the ground for firm grip and thus arrest the toppling of winch. The design of the toppling arrester takes into consideration the tether tension at drum location for all possible movement patterns of the aerostat due to ambient wind conditions. Further, the winch is powered by a single phase induction motor that drives a pulley system which in turn drives the gear pairs for rotating the main tether

drum during recovery. A separate drum has also been provided to release and wind a data cable from the ground to a payload mounted on the aerostat which could be a communication system, still/ video camera or a data logger etc. This drum is also powered by an inversion of four bar link mechanism that draws power from main drum shaft.

III. Effect of envelope shape on an aerostat's payload capacity

The envelope shape affects the payload capacity in many ways. The envelope weight is decided by the Total Surface Area (TSA) of the envelope, which, for a given envelope volume, can vary greatly with its shape. The difference in internal and external pressure on the aerostat envelope generates stress on the membrane. For a given pressure difference, the stress is a function of the envelope shape. If the stress is low, a material of low ultimate strength can be used, which is expected to be lighter. On the other hand for a higher stress, a stronger material which is expected to be heavier (due to higher ρ_{matl}) will have to be used. Thus shape directly influences the self weight of the aerostat. The envelope shape also decides the aerodynamic force and moments generated on it. The size of fins required to trim the aerostat at a given angle of attack and to provide the required stability is thus a function of its shape. The ambient wind on the aerostat produces drag which tends to displace it along the direction of flow. This displacement is called blow-by, and it reduces the operational height of an aerostat and may also give rise to functional disadvantages depending on the application, for instance, to maintain the specified altitude of operation; a longer tether will have to be released at the expense of a decrease in payload capacity. To increase the payload capacity, it is thus necessary to reduce the envelope drag coefficient C_D.

IV. Previous study in aerostat envelope shape optimization

In a previous study by Kanikdale et al.[13], the envelope geometry of an aerostat was parameterized using a sphere for the nose, two cubic splines for the mid-body and a parabola for the rear, as shown in Figure 9.

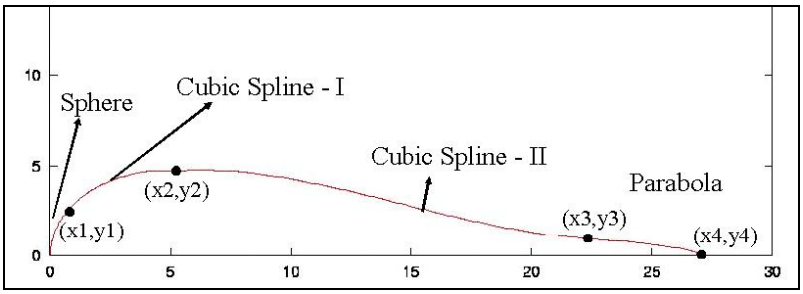

Figure 9. Parameterization of geometry[1]

The defining equations for the various shape segments are given in Eqns. (5-8).

Sphere (Circle in 2-D): $y^2 = 2xR - x^2$ (5)

Spline I: $y = a_1 x^3 + b_1 x^2 + c_1 x + d_1$ (6)

Spline II: $y = a_2 x^3 + b_2 x^2 + c_2 x + d_2$ (7)

Parabola: $y^2 = a_n (x_4 - x)$ (8)

By imposing constraints on the slope continuity at points (x_1, y_1), (x_2, y_2) and (x_3, y_3), and zero slope at point (x_2, y_2) for an aerostat envelope of fixed volume, the size of the design vector was reduced to six,

viz., $X_D = (x_1, y_2, x_2, x_3, y_3, x_4)$. Additional constraints on the radius of curvature and rate of change of slope were also employed to incorporate manufacturing constraints. A shape generation algorithm was developed, which generated various possible shapes of aerostat envelopes by varying these geometrical parameters, while meeting the specified constraints.

An objective function F_{comp} incorporating the disciplines of Aerodynamics (through Volumetric Drag Coefficient C_{DV}), and Structures (through Envelope Surface Area S, and Max. stress σ_{max}) was formulated as:

$$F_{comp} = w_1\left(\frac{C_{DV}}{(C_{DV})_{GNVR}}\right) + w_2\left(\frac{S}{S_{GNVR}}\right) + w_3\left(\frac{\sigma \max}{\sigma_{GNVR}}\right) \quad (9)$$

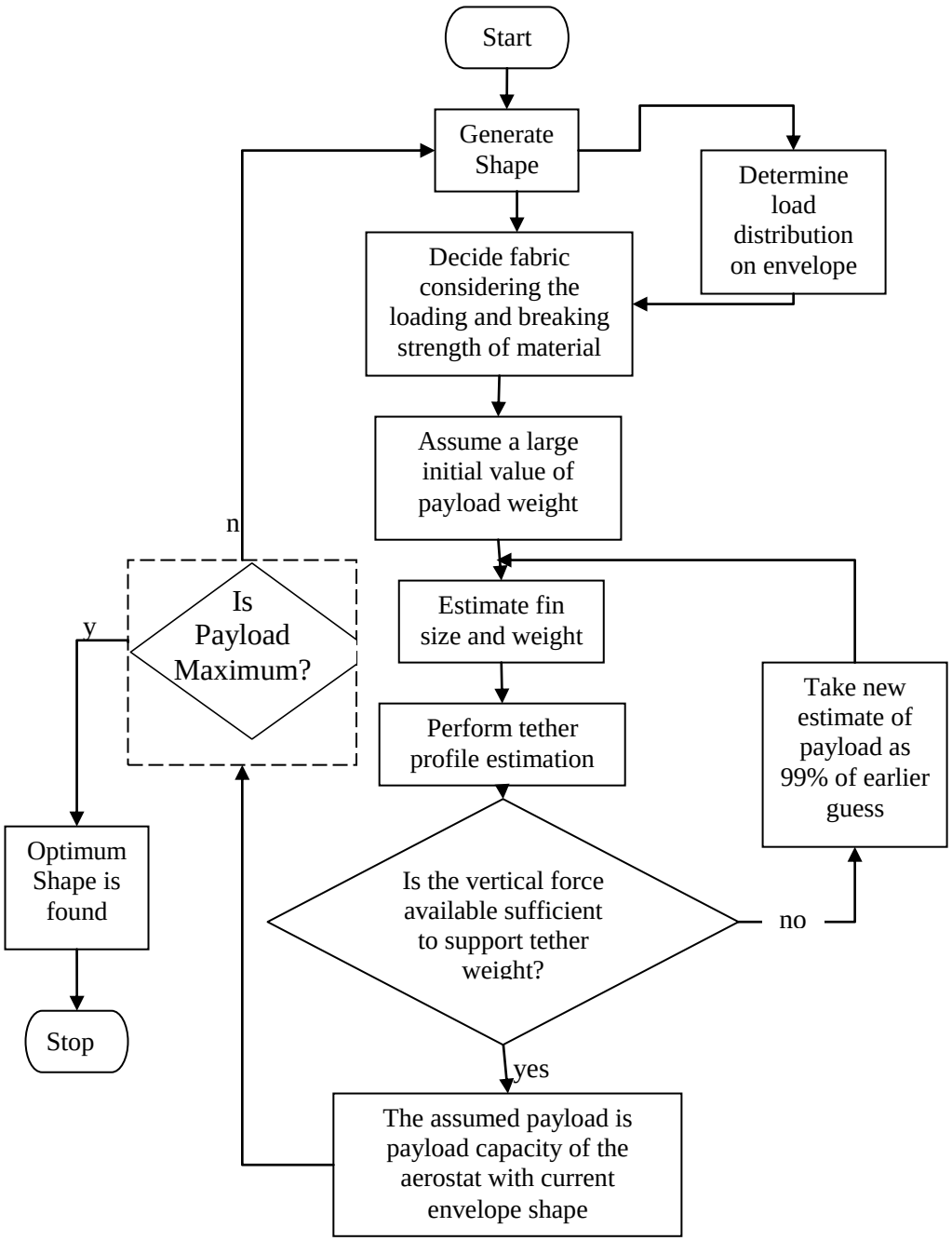

Figure 10. Methodology for Shape Optimization

Where w_1, w_2 and w_3 are user-specified weight functions. The subscript GNVR in the quantities listed above refer to the corresponding values of these parameters for a reference GNVR shape. The optimum shape for various values of weight functions was obtained by coupling the shape generation algorithm to an optimizer. In the present work, the GADO (Genetic Algorithm for Design Optimization) code developed by Rasheed[14] has been coupled to the shape generation algorithm to obtain the envelope shape that maximizes the payload capacity. Figure 10 shows the methodology adopted for solving the problem.

In order to eliminate the need of using a flow solver for determination of C_{DV} in all iterations of the optimization process, a co-relation between C_{DV} and some geometry related parameters is required. Such an empirical formula was developed for an aerostat of envelope volume 1000 m^3 and a length of 26.26 m, by computing C_{DV} for a number of envelope shapes. Aerodynamic analyses were carried out using FLUENT™ flow solver package. An axi-symmetric, solver was used in conjunction with S-A turbulence model. Figure 11 shows the structured grid around a trial envelope shape and the semi-circular domain that was used.

In this study, the envelope length was kept fixed to avoid compromising on stability with respect to the reference GNVR shape. However, it is a known fact that the size of the fins can be greatly reduced if the envelope length is increased, which results in a larger payload. Secondly, the formulation used in Kanikdale et. al[13]'s model was not amenable to coupling with an MDO process, since it requires detailed geometric data about the envelope shape, especially the co-ordinates of several points at the nose and trailing edge, and the grid density in these regions. The co-relation was arrived using some arbitrarily derived coefficients, purely based on observation of the flow patterns.

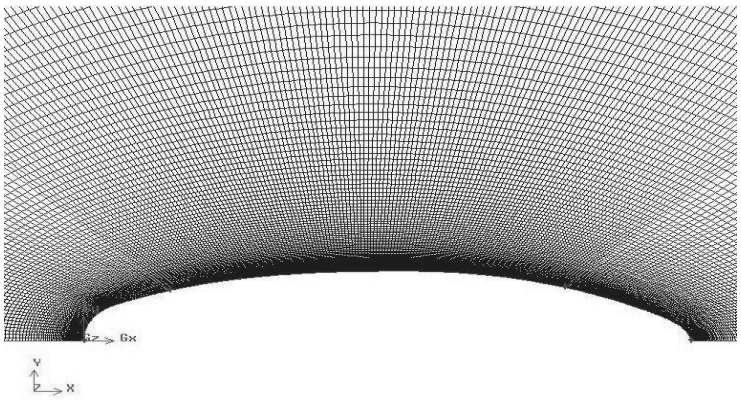

Figure 11. Structured grid around Aerostat envelope in a semicircular domain

V. Details of present study

In the present work a more generic expression[15] to estimate C_{DV} is used, which is a function only of the six geometrical parameters. The problem is formulated to maximize payload. The drag on the aerostat envelope and the stresses generated are expressed in terms of the penalty that they impose on payload capacity of the aerostat. The weight of the fins required for stability is estimated to accurately predict the payload capacity. Unlike in the previous study, the length of the aerostat has also been kept as a free variable, since appropriate restrictions have been inserted on the length by requirement on the size of fin.

The drag on an aerostat produces *blowby* or lateral displacement, due to which either a longer tether is required to maintain a particular operational height, or there is a decrease in operational height of the aerostat, for a given tether length. The added weight of the tether decreases the payload capacity. To obtain a correct

estimate of the payload capacity, the tether profile and weight for a given drag coefficient is obtained using the methodology suggested by Wright[16]. In this method, the tether is discretized into small elements of equal lengths, starting from the confluence point. The tension and angle of inclination of each of these elements are determined by considering the equilibrium of forces on them.

K. Methodology for Sizing of Fins of an Aerostat

Fins are required for the stability of the aerostat, but they also constitute a major portion of the weight and also add to the drag. In order to accurately estimate the payload capacity of the aerostat, the size and weight of the fins that would be required for adequate stability are estimated. A methodology for sizing the inverted Y-shaped fins of a tethered aerostat has been developed, in which the stability analysis is based on the approach suggested Krishnamurthy & Panda[17].

An inverted Y configuration is selected for the fins so that rain and snow falling on the fins does not accumulate on the fins thus avoiding disturbance to the balance of the aerostat. The coordinates of the confluence point $(\overline{x_c}, \overline{z_c})$ for a given size of fin can be obtained and thus the stability margin C_{m_α} taken about the confluence point can be obtained. The aspect ratio, taper ratio and location of the fin along the hull are initially assumed. The fin area required for adequate stability is determined through an iterative process. Starting from a small initial guess, the fin area is increased till the confluence point is at an acceptable location. If the aerostat has sufficient static margin for the given fin size and confluence point, it is accepted. Empirical co-relations for aerodynamic coefficients suggested by Jones and De-Laurier[18] for symmetric fin configuration, and Malik, Gill and Pant[19] for un-symmetric Y-fin configuration are utilized in this methodology.

L. Envelope Weight Estimation and Structural Considerations

The self-weight of the hull is estimated as a function of the weight of the envelope fabric. The weight of the fabric of the envelope depends on the surface area of the aerostat and the density of the material used. The material used for the construction of the envelope should be strong enough to withstand the loads developed due to the internal pressure of the gas inside the aerostat, and the dynamic loads imposed due to the ambient wind. Structural considerations in the present study involve estimating the hoop and bending stress developed in the envelope.

M. Aerostat Envelope Weight Reduction by Multi fabric Construction

In order to maximize the payload of the aerostat, the self-weight of the aerostat should be reduced to the extent possible. The load on the fabric is not uniform throughout the fabric. The hoop stress of the aerostat envelope is obtained from eq. 4.

This equation shows that regions with a larger diameter in the middle of the aerostats are more loaded and regions of smaller diameter near the ends of the aerostat are lightly loaded. Hence a great advantage in terms of payload capacity of the aerostat can be achieved if the front and rear of the aerostat are made with lighter materials of comparatively low strength and the middle regions are made with high strength (but comparatively heavier) material as shown in Figure 12 rather than using the same material for the entire aerostat.

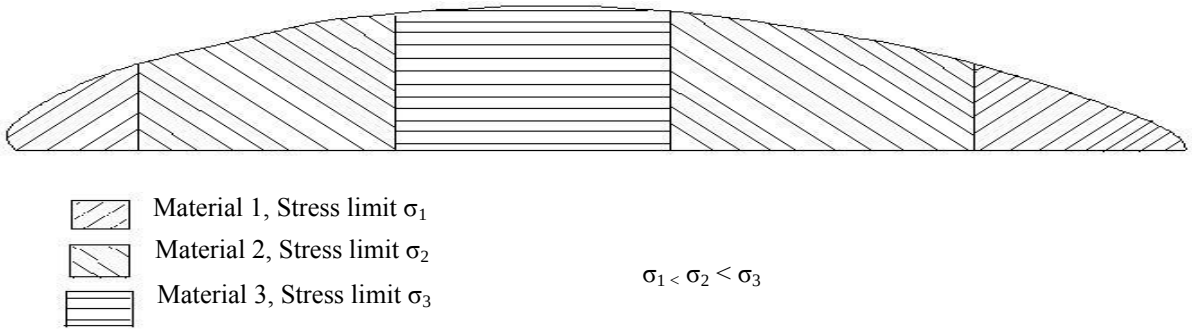

Figure 12. Multi-fabric construction of the aerostat envelope

The fabric to be used for each portion of the aerostat and the fabric weight of the aerostat were estimated based on the values of load acting per unit length along the meridians (warp direction) and along latitude circles (weft). Considering a suitable factor of safety, a fabric having breaking strength just higher than the tensile force developed will be used for that particular portion.

The breaking strength of a fabric is generally reported in terms of load per unit width. Typical data related to the load per unit width for three fabrics, and their respective specific weights used in this study are listed in Table 3.

Table 3. Material Properties of aerostat fabrics

Properties	**Fabric # 1**	**Fabric # 2**	**Fabric# 3**
Specific Mass (g/m^2)	280	340	385
	Breaking Strength (kN/m)		
Warp direction	15	30	45
Weft direction	14	30	45

Using this data, the envelope profile for minimum fabric weight, employing a multi fabric construction of the envelope was obtained. The shape of the envelope was optimized for minimum fabric weight using a multi fabric approach. It was found that for a factor of safety of 4, the maximum load on the material was lower than the design breaking strength for Fabric # 2. Thus, Fabric # 3 is not required for this shape. A saving of ≈ 20 kg was obtained in the fabric weight using multi fabric construction, as compared to an envelope of single fabric construction using Fabric # 1, which represents a 6.5% savings in fabric weight, which can directly be translated into increase in payload. The methodology has been employed for an aerostat of 2000 m^3, and various solutions for multi-fabric envelope configurations have been obtained.

N. Results Obtained

The payload capacity of an aerostat having a GNVR shaped envelope was estimated for a single and multiple fabric construction. The fabric distribution in the multi fabric construction is as shown in Figure 13.

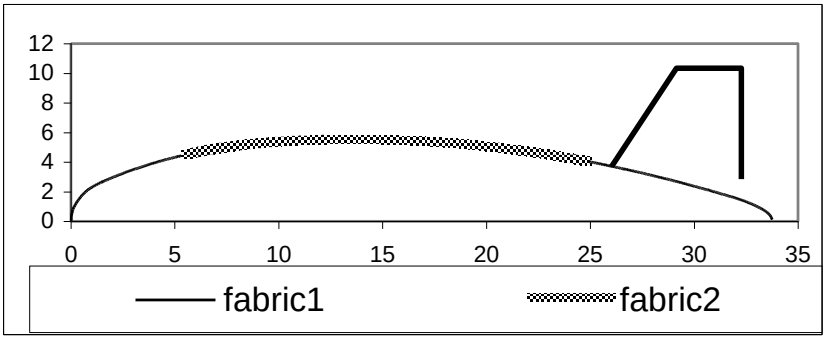

Figure 13: Fabric distribution for multi-fabric GNVR shaped aerostat

The weight breakup calculated for the single fabric and multi-fabric construction is given in Table 4.

Component Weight	Single fabric (kg)	Multi-fabric (Kg)
Payload (Kg)	237.4	286.4
Fin (Kg)	107.8	75.4
Envelope Membrane (Kg)	309.4	293.6
Tether Force (Kg)	735.1	734.4
Location of Confluence point		
x_c (from nose) (m)	11.4	6.9
z_c (m)	11.6	10.6

Table 4. Properties of single and multi-fabric GNVR shaped aerostats

O. Optimum Shape for Single Fabric Construction of Aerostat

The four optimum shapes of single fabric aerostats were determined using the GA based optimizer GADO are shown in Figure 14.

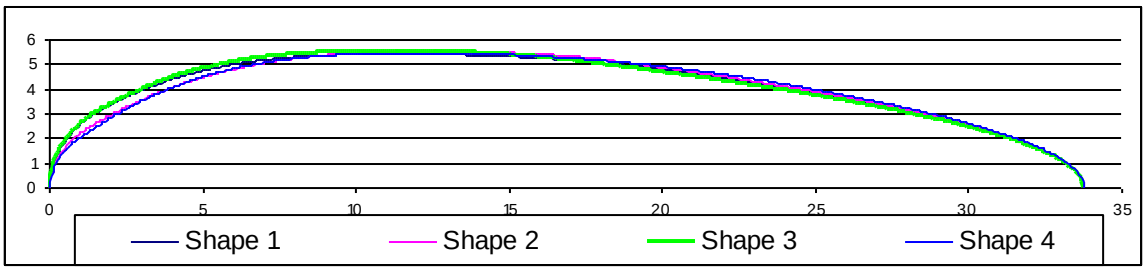

Figure 14 Optimum shapes of single fabric aerostat envelopes

The weight breakup of these shapes is given in Table 5. It can be seen that while all these shapes have almost the same payload carrying capacity, Shape 2 has the maximum. This shape has the least surface area, hence the least envelope weight. The low surface area also reduces the drag on the shape, hence the force required to lift the tether is also low.

Profile	Payload (Kg)	Fin (Kg)	Envelope Fabric (Kg)	Tether Force (Kg)
Shape 1	241.9	99.2	312.2	736.5
Shape 2	242.5	102.1	310.5	734.7
Shape 3	242.2	97.9	311.5	738.2

Shape 4	240.5	102.4	310.8	736.1

Table 5. Weight break up of single fabric Aerostats

The profile of the shape along with the fin is shown in Figure 15. It's confluence point is located at x_c'= 10.8m behind the nose and z_c= 11.1 m below the axis, which is an acceptable position.

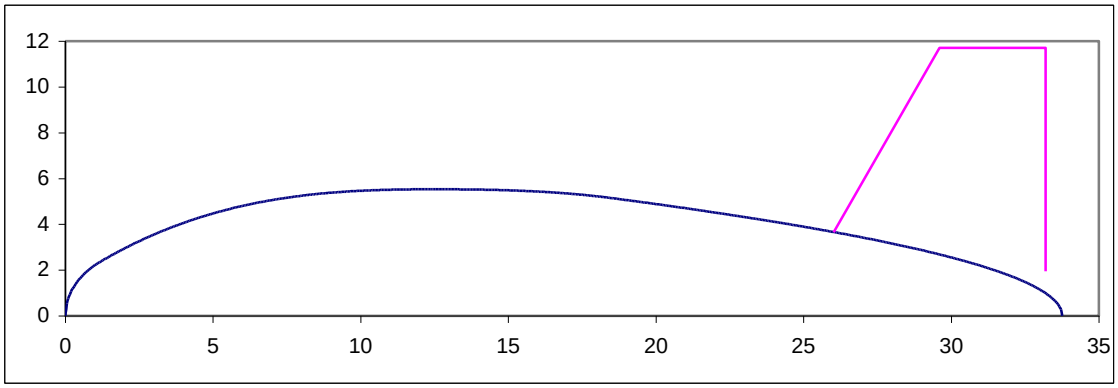

Figure 15. Best envelope shape for single fabric construction of Aerostat

P. Optimum Shape for Multi Fabric Construction of Aerostat

The optimum shapes for a multi-fabric aerostat obtained from four different runs of GADO optimizer are shown in Figure 16. These shapes result in considerable reduction in weight of envelope fabric weight and fin but the confluence point is located close to the nose (as fabric distribution moves the CG backwards) which is not an acceptable position. The confluence point can however be maintained at any desired position by adjusting the position of the payload and consequently the CG of the aerostat.

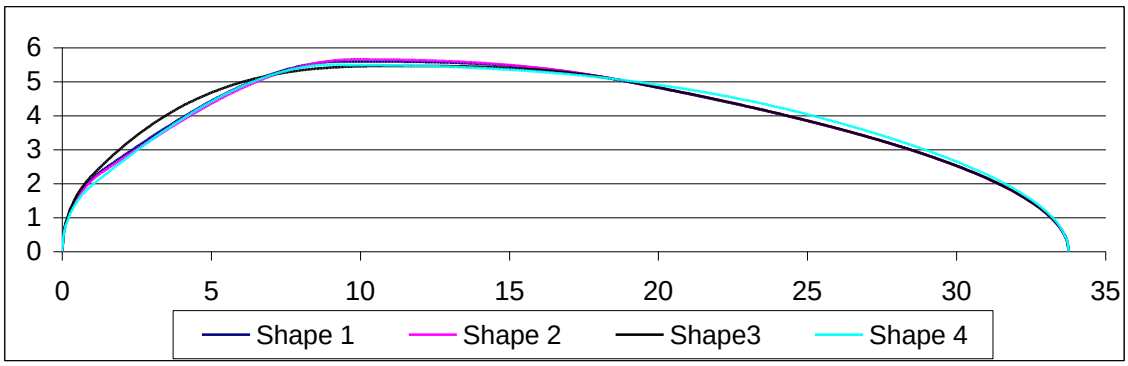

Figure 16. Optimum shapes for multi fabric aerostats

Table 4 gives the weight breakup of the four different multi-fabric shapes obtained through optimization. It can be seen that while all these shapes have almost the same payload capacity, but Shape 1 has the maximum.

Table 6. Weight Breakup for Multi Fabric Shapes

Profile	Payload capacity (Kg)	Envelope fabric weight (Kg)	Fin weight (Kg)	Tether force (Kg)
Shape 1	296.2	288.2	69.1	736.2
Shape 2	294.3	290.0	69.3	736.2
Shape 3	293.1	293.2	69.3	734.2

Shape 4	295.1	287.2	69.5	737.9

The profile of this aerostat along with the fin size is shown in Figure 17. The thick jagged line shows regions in which the stronger fabric is used. The shape shown in Figure 17 has a maximum diameter of 11.2 m. The ideal position of the confluence point for this shape is x_c'=11.2 m behind the nose and z_c = 11.2 m below the axis. By adjusting the CG of the aerostat shown, if the confluence point was brought near to the desired location, the new weight breakup and the confluence point location are as listed in Table 7.

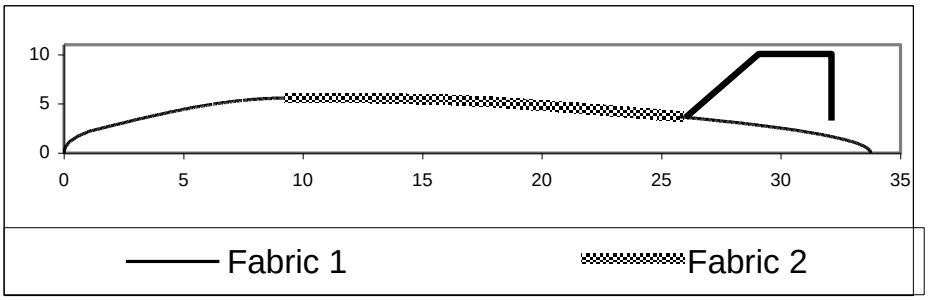

Figure 17: Multi-fabric aerostat having highest payload capacity

Table 7: Multifabric envelope properties after CG adjustment

Payload Capacity (Kg)	Fin weight (Kg)	Fabric weight (Kg)	Tether force Kg)	x_c' (m)	z_c (m)
252.7	110	288.2	738.2	10.8	12.7

It can be seen that the payload capacity was still nearly 11 Kg (≈4.5%) greater than that for the most optimum single fabric envelope.

Q. Sensitivity Analyses

Sensitivity of the payload capacity of the aerostat to operating conditions and design requirements has also been studied. In all the studies, the input parameter was varied in the range of ±10% from the design condition for the most optimum single fabric aerostat (shown in Figure 14) and the effect on payload capacity studied. It was observed that payload capacity decreases considerably with increase in fabric density, and tether weight per unit length due to increased self weight. The payload capacity also decreases slightly with change in angle of attack. With reduction in angle of attack, fin sizes required are considerably high. The fin weight and the location of confluence point depend to a great extent, on the location of CG. Backward movement of the CG causes the fin size to decrease but moves the confluence point forward to an undesirable position.

VI. Summary and Conclusions

Most studies on aerostat envelope shapes are carried out on the basis of aerodynamic considerations. However, an aerostat being primarily a payload carrying device, its efficacy depends on its net payload carrying capacity. Aerodynamic analysis is carried out using a semi-empirical method. The Envelope drag at zero angle of attack is determined using a response surface. A methodology has been developed for sizing the fins of the aerostat. Methods to determine the weight of the tether to be carried by the aerostat have also been employed in

order to study the effect of drag on the payload capacity of the aerostat. The shape generation algorithm proposed by Kanikdale et al.[14] has been made more robust by introducing a new constraint to avoid kinks and folds to develop on the shape. Shapes have been generated using the shape generation algorithm and a GA based optimizer GADO used to determine the most optimum shape using single and multi-fabric construction. The payload of an aerostat of the GNVR shape has been estimated for a single fabric and multi-fabric construction. The payload capacity of the optimum shape of single fabric construction was found to be ~ 2.2 % higher compared to a similar envelope using the standard GNVR shape. However, use of multi-fabric construction was seen to increase the payload capacity by ~ 22% for both the GNVR and optimum shape. This was obtained at the expense of moving the confluence point away from its desired position due to shift in the centre of gravity. Sensitivity of the payload capacity of the aerostat to different operating conditions and design requirements has been studied.

Acknowledgements

This study was carried out as part of an R&D project sponsored by ADRDE. The author would like to thank Mr. M. L. Sidana, ex-Director, Mr. K. K. Thaper, Sc. G., Mr. Sudhir Gupta, Sc. F, Mr. Sandeep Malik, Sc. D, and Mr. Puneet Gupta, Sc. B for advice, suggestions, fruitful discussions and interactions during the execution of this project. The help and advice rendered by Prof. A. G. Marathe, IIT Bombay on use of FLUENT™ and Prof. G.N.V. Rao, Prof. M. Krishnamurthy, and Prof. K. Sudhakar, and Dr. Sekhar Majumdar, NAL on the aerodynamics and flight mechanics procedures used is also gratefully acknowledged. Thanks are also due to the various project engineers, viz., Mr. Amol Gawale, Mr. Sagar Kale, Mr. Pankaj Joshi, and students, viz., Mr. Tushar Kanikdale and Mr. C. Vijayram who carried out parts of this study as part of their M. Tech. dissertation.

References

[1]Gupta, P., Pant. R. S., A methodology for initial sizing and conceptual design studies of aerostats", *International Seminar on Challenges in Aviation Technology, Integration and Operations (CATIO-05)*, Technical Session of 57th Annual General Meeting of The Aeronautical Society of India, December 2005.

[2]Raina, A. A., Gawale A. C., Pant, R. S., "Design, Fabrication and Field Testing of Aerostat system", *National Seminar on Strategic Applications of Lighter- Than- Air (L-T-A) Vehicles at Higher Altitudes*, Snow and Avalanche Study Establishment, Manali, India, 12-13 October 2007

[3]Anderson, J. D., (Jr), "Introduction to Flight", McGraw-Hill Book Company, New York, USA, 3rd ed., Chaps. 2, 3, 1989.

[4]Khoury, G. A., and Gillett, J. D., "Airship Technology", Cambridge University Press, Cambridge, UK, 1st ed., 1999.

[5]Hoerner, S. F., "Fluid Dynamic Drag," Midland Park, New Jersey, pp. 11.1-11.4 and pp. 44.1-44.2, 1957.

[6] Gupta, S., Malik, S., "Envelope details for Demo Airship", Aerial Delivery Research and Development Establishment (ADRDE), Agra, January 2002

[7]Greschner, B., Yu.,C., Zheng, S., Zhuang, M., Wang, Z., J., and Thiele, F., "Knowledge Based Airfoil Aerodynamic and Aero-acoustic Design", AIAA Journal, URL: http://www.public.iastate.edu/~zjw/papers/AIAA-2005-2968.pdf [Cited in March 2006].

[8]Mason, W., H., "Subsonic Aerodynamics of Airfoils and Wings"

[9]David, C., Graham, W., Smith, T., "Inflatable and Rigidizable Wings for Unmanned Aerial Vehicles", ILC Dover, Inc., Frederica, DE, USA. URL: http://www.ilcdover.com/products/aerospace_defense/supportfiles/AIAA2003-6630.pdf [cited March 2006]

[10]Wright, J., B., "Computer Programs for Tethered-Balloon System Design and Performance Evaluation", Report No. AFGL-TR-76-0195. Air force Geophysics Laboratories (LCB) Hanscom AFB, Massachusetts 01731, August 1976.

[11] Sequeira, G. A., Bhandari, K., Wanjari, N., Kadam, S., Sapkal, S., "Design, Fabrication and Field testing of Winch for Aerostat", *National Seminar on Strategic Applications of Lighter- Than- Air (L-T-A) Vehicles at Higher Altitudes*, Snow and Avalanche Study Establishment, Manali, India, 12-13 October 2007 (to be published).

[12]Michael Markey, "Handbook of Oceanographic Winch", 3rd Ed., Wire and Cable Technology, Chap. Single Drum Winch Design.
URL:http://www.unols.org/publications/winch_wire_handbook__3rd_ed/10_single_drum_winches.pdf [cited in May 2006]

[13]Kanikdale, T. S., Marathe, A. G., and Pant, R. S., "Multidisciplinary Optimization of Airship Envelope Shape", AIAA-2004-4411, Proceedings of 10th AIAA/ISSMO Multidisciplinary Analysis and Optimization Conference, Albany, USA, 2004.

[14]Rasheed K. M., "GADO: A Genetic Algorithm For Continuous Design Optimization", Ph.D. Dissertation, Graduate School, New Brunswick Rutgers, The State University of New Jersey, January, 1998.

[15]Kale S. M., Joshi P., Pant R. S., "A Generic Methodology to Estimate Drag on an Aerostat Envelope", *Proceedings of AIAA 5th Aviation Technology, Integration, and Operations Conference (ATIO) and 16th Lighter-Than-Air Systems Technology Conference and Balloon Systems Conference*, September 2005, Arlington, USA.

[16]Wright J. B., Computer programs for tethered-Balloon System Design and Performance Evaluation, Report No. AFGL-TR-76-0195, Air Force Geophysics Laboratories (LCB) Hanscom AFB, Massachusetts 01731, August 1976.

[17]Krishnamurthy M., Panda G.K., "Equilibrium Analysis of a Tethered Aerostat", Project document FE 9802, Flight Experiments division, National Aerospace Laboratories, November 1998.

[18]Jones S. P., Delaurier J. D., "Aerodynamic Estimation Techniques for Aerostats and Airships", American Institute of Aeronautics and Astronautics, Report No. 81-1339, 1981.

[19]Gill P., Malik S., Pant R. S., "Estimation of Aerodynamic Characteristics of Un-Symmetrically Finned Bodies of Revolutions", *Proceedings of 28th Fluid Mechanics & Fluid Power Conference*, Chandigarh, India, December 2001.